

# Enigma: Privacy-Preserving Execution of QAOA on Untrusted Quantum Computers

Ramin Ayanzadeh<sup>1</sup>, Ahmad Mousavi<sup>2</sup>, Narges Alavisamani<sup>1</sup>, and Moinuddin Qureshi<sup>1</sup>

<sup>1</sup>School of Computer Science, Georgia Institute of Technology, Atlanta, GA

<sup>2</sup>Department of Mathematics and Statistics, American University, Washington, DC

**Abstract**—Quantum computers can solve problems that are beyond the capabilities of conventional computers. As quantum computers are expensive and hard to maintain, the typical model for performing quantum computation is to send the circuit to a quantum cloud provider. This leads to privacy concerns for commercial entities as an untrusted server can learn protected information from the provided circuit. Current proposals for *Secure Quantum Computing (SQC)* either rely on emerging technologies (such as quantum networks) or incur prohibitive overheads (for Quantum Homomorphic Encryption). The goal of our paper is to enable low-cost privacy-preserving quantum computation that can be used with current systems.

We propose *Enigma*, a suite of privacy-preserving schemes specifically designed for the *Quantum Approximate Optimization Algorithm (QAOA)*. Unlike previous SQC techniques that obfuscate quantum circuits, Enigma transforms the input problem of QAOA, such that the resulting circuit and the outcomes are unintelligible to the server. We introduce three variants of Enigma. *Enigma-I* protects the coefficients of QAOA using random phase flipping and fudging of values. *Enigma-II* protects the nodes of the graph by introducing decoy qubits, which are indistinguishable from primary ones. *Enigma-III* protects the edge information of the graph by modifying the graph such that each node has an identical number of connections. For all variants of Enigma, we demonstrate that we can still obtain the solution for the original problem. We evaluate Enigma using IBM quantum devices and show that the privacy improvements of Enigma come at only a small reduction in fidelity (1%–13%).

## I. INTRODUCTION

Quantum computers (QCs) have the potential to solve certain problems that are beyond the capability of classical computing [4], [66], [72], [89], [90], including optimization [37], machine learning [52], cryptography [79], and quantum simulation [39]. Unlike classical systems, QCs require highly sophisticated infrastructure and maintenance; thus, quantum users are expected to run their quantum programs on remote QCs accessible via the cloud. However, disclosing quantum programs in the form of a quantum circuit to the server raises security and privacy concerns, as untrusted cloud providers can infer sensitive data, including intellectual property.

When we use QCs to solve a problem, the algorithm for this problem must be adapted to the quantum computing framework. In circuit-based quantum computing, for instance, the algorithm is represented using quantum gates and circuits. To execute these algorithms, users typically rely on cloud services, which run these quantum circuits on remote QCs. This process, however, reveals the quantum circuit—and potentially

sensitive details about the problem and its solution—to the cloud service providers. This is particularly concerning for future quantum computing applications, where the problems being solved are those that classical computers cannot handle. These problems often involve highly sensitive data, such as drug discovery [22], [25], [34], [40], [74], [76] or financial optimization [13], [15], [18], [32]. Therefore, a substantial privacy risk exists: untrusted cloud servers may access and misuse sensitive information about advanced technologies and strategies in sectors such as pharmaceuticals and finance. This presents a major privacy concern for companies looking to leverage quantum computing.

*Secure Quantum Computing (SQC)* is an emerging field that aims to address security and privacy concerns arising from the delegation of quantum programs to untrusted remote servers. SQC techniques are broadly categorized into *Blind Quantum Computing (BQC)* and *Quantum Homomorphic Encryption (QHE)*. BQC protocols partially delegate quantum programs without disclosing the computation’s details to the server [16], [20], [42], [55]. However, current BQC protocols are often impractical as they typically assume the client has basic quantum hardware to prepare quantum states, which in turn requires a quantum network for client-server interactions—a technology that is still under development. Recent updates to BQC reduce the need for users to have their own quantum capabilities [42], [44], [45], [51], [62], [73]. However, these still need multiple servers and rely on the assumption that these servers do not collaborate in a way that compromises privacy. Yet, this assumption is often not reasonable given that we are dealing with *untrusted* servers. QHE schemes, on the other hand, enable computations on encrypted quantum data, producing an encrypted outcome. Once decrypted, this outcome reflects the results of operations on the original data [19], [21], [31], [41], [56], [68], [83], [91]. However, QHE remains impractical in the near term as fully secure QHE methods impose an exponential computational overhead.

The near-term impracticality of previous work arises from their pursuit of a one-size-fits-all approach to protect the privacy of any quantum program, which forces reliance on emerging technologies or results in exponential computing overhead. In this paper, we advocate for *application-specific SQC*, tailoring SQC schemes for immediate use on current and near-term quantum computers, albeit with a focused scope on a single, yet significant, application. This approach

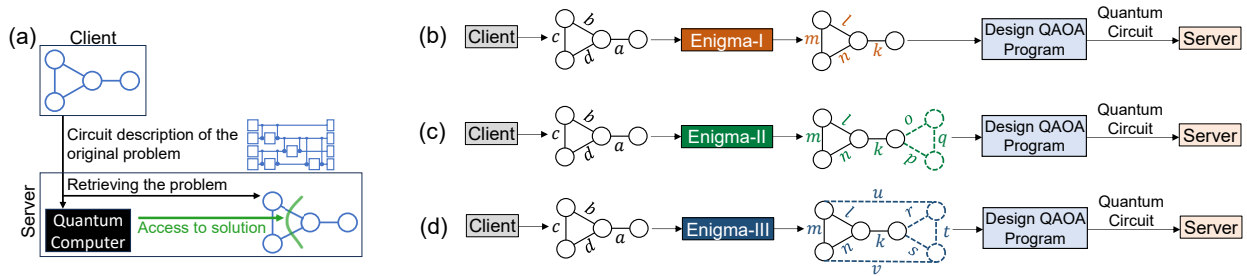


Fig. 1. (a) Untrusted servers can deduce the original QAOA problem from the circuit and solution. Enigma obfuscates the QAOA problem, rendering the input problem and circuit outcomes inaccessible to the server: (b) Enigma-I conceals the problem coefficients; (c) Enigma-II introduces decoy qubits to alter the problem structure; (d) Enigma-III regularizes the problem graph.

represents a strategic trade-off between breadth of application and deployment readiness.

Optimization leads the applications poised to demonstrate quantum speedup on *Noisy Intermediate-Scale Quantum (NISQ)* computers [72], with the *Quantum Approximate Optimization Algorithm (QAOA)* [17], [37], [38] as a prime contender. QAOA’s objective is to find the lowest energy state of a system, known as the Hamiltonian. It shows promise for various industrial applications aimed at optimizing specific cost functions [24], [25], [27], [81], [88].

However, QAOA is particularly vulnerable to privacy breaches as its distinctive circuit design can easily reveal details about the problem being solved. For example, when addressing graph optimization problems, QAOA translates the graph into a quantum circuit where nodes become qubits and edges are represented by two-qubit gates linking the relevant qubits. As depicted in Fig. 1(a), the circuit’s unique layout could disclose the graph’s structure, allowing untrusted servers to glean the intellectual property embedded within the user’s problem. Such exposure jeopardizes the confidentiality of the original problems users are tackling. Furthermore, when QAOA circuits are run on the cloud, cloud service providers gain access not just to the problem but also to its solution, presenting a substantial risk of IP leakage as providers could potentially access both the problem and its solution (Fig. 1(a)).

In this paper, we propose *Enigma*, a suite of privacy-preserving schemes tailored specifically for QAOA applications. The Enigma protocols encode optimization problems into forms unintelligible by servers. Clients submit obfuscated problems whose output distributions can only be decoded by them. QAOA involves three types of assets: coefficients, variables, and the problem graph’s structure. We introduce three protocols to conceal these elements. Our experiments show that Enigma can obfuscate problems and decode outcomes for QAOA instances with hundreds of qubits in just a few seconds.

We propose *Enigma-I*, Fig. 1(b), which encrypts problem coefficients, effectively obfuscating both the input and outcomes. While Enigma-I maintains the energy levels of the input Ising Hamiltonian, it permutes the associated bitstrings, rendering the outcomes unintelligible to the server.

Although Enigma-I ciphers coefficients, it leaves the problem’s structure, such as the number of nodes and edges still unprotected and visible to the server. We introduce *Enigma-II*, as shown in Fig. 1(c), to further perturb the problem structure

by integrating decoy qubits, making them indiscernible to the server. Enigma-II ensures the recovery of the problem of interest from the obfuscated problem’s global minimum.

However, merely embedding decoy qubits does not completely obscure the problem graph’s structure. For example, when addressing problems that follow a power-law distribution, certain qubits—known as hotspots—may exhibit significantly more connections, thereby becoming easily identifiable to the server (for example, if the problem graph had airport routes, then Atlanta and Chicago would have a large number of connections and would still be identifiable even with Enigma-II). To comprehensively conceal the problem’s structure, we introduce *Enigma-III*, as shown in Fig. 1(d). Enigma-III embeds the required number of decoy qubits and connections so that all qubits have an identical number of connections, resulting in a regular graph for the obfuscated problem.

For each scheme, we present analytical evaluations of the protective measures for QAOA assets and discuss residual risks. We also provide experimental results based on IBM quantum devices to evaluate the effectiveness. To the best of our knowledge, Enigma is the first SQC proposal that does not depend on nascent technologies like those in BQC and avoids the exponential computational overhead associated with QHE, thus making it readily deployable even on existing and near-term quantum systems that cannot perform error correction.

Overall, this paper makes the following contributions:

- 1) We propose *Enigma* as a SQC protocol specifically designed to protect the privacy of QAOA programs at the application layer. To the best of our knowledge, Enigma is the first application-specific SQC proposal.
- 2) We propose *Enigma-I*, a protocol that encrypts problem coefficients, leading to random bit flips in outputs, effectively concealing both the coefficients and the outcomes.
- 3) We propose *Enigma-II*, a protocol that modifies the graph structure by including a number of decoy qubits.
- 4) We propose *Enigma-III*, a protocol that hides the connectivity information by transforming the graph to have an identical number of connections for all nodes.

Enigma can be deployed on current and near-term machines. Our evaluations with IBM quantum machines shows that the privacy enhancements of QAOA comes at only a small loss of fidelity: 1% for Enigma-1 to 13% for Enigma-III.

## II. BACKGROUND AND MOTIVATION

### A. QAOA: A Prime Quantum Speedup Candidate

The Quantum Approximate Optimization Algorithm (QAOA) [17], [37], [38] is widely recognised as the prime candidate for demonstrating quantum speedup in Noisy Intermediate-Scale Quantum (NISQ) era [72]. To solve a problem using QAOA, we must cast it into the following Ising Hamiltonian:

$$f(\mathbf{z}) = \sum_{i=1}^n \mathbf{h}_i \mathbf{z}_i + \sum_{i=1}^n \sum_{j=i+1}^n J_{ij} \mathbf{z}_i \mathbf{z}_j + \text{offset}, \quad (1)$$

characterized by spin variables  $\mathbf{z}_i \in \{-1, +1\}$  and associated linear ( $\mathbf{h}_i \in \mathbb{R}$ ) and quadratic ( $J_{i,j} \in \mathbb{R}$ ) coefficients that are defined such that the global minimum of the quadratic objective function corresponds to the optimal solution of the problem at hand [5], [6], [8], [59].

As shown in Fig. 2(a), the Ising Hamiltonian is represented as a “problem graph”, where nodes correspond to spin variables and edges to quadratic terms. The, this graph is transformed into a parametric quantum circuit (Fig. 2(b)), with each node and edge represented by qubits and quantum gates (two CNOTs and one  $R_z$ ), respectively. Parameters ( $\gamma$  and  $\beta$ ) are optimized using an external classical optimizer to align the circuit’s output with the problem’s optimal solution. Importantly, as depicted in Fig. 2, the structure of the QAOA circuit closely mirrors the original problem graph.

### B. Why QAOA?

Optimization is at the forefront of showcasing quantum speedup with near-term quantum devices. Meanwhile, QAOA stands out as a prime candidate to surpass classical computing capabilities by approximating global optima in optimization tasks. Moreover, QAOA is computationally universal [58], [63], enabling us to employ it for addressing a vast range of problems beyond the optimization realm [11], [59], [69]. We can anticipate QAOA to be among the first real-world applications of quantum computing, underscoring the urgency to prioritize the security and privacy of its users.

### C. Prior Work Limitations

1) *Blind Quantum Computing (BQC)*: BQC is a method that allows a client to perform quantum computations on a remote server while keeping the computation’s content confidential. The main objective of BQC is to maintain the privacy of the quantum computation, ensuring that the server, although performing the computation, cannot ascertain its nature or purpose. However, most BQC protocols operate under the assumption that the client possesses a rudimentary quantum device and that a quantum network is in place to facilitate communication between the client and the server [20], [23], [42], [43], [55], [64].

Recent studies have proposed BQC protocols that eliminate the need for clients to host a quantum device on their premises [42], [44], [45], [51], [62], [73]. However, these protocols rely on the presence of multiple quantum servers

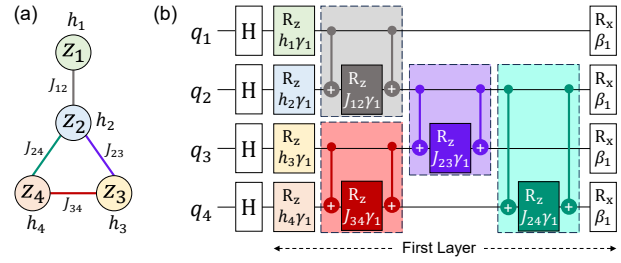


Fig. 2. QAOA example: (a) the problem graph of an Ising Hamiltonian with four spin variables, featuring associated linear ( $\mathbf{h}$ ) and quadratic ( $J$ ) coefficients; and (b) the corresponding QAOA circuit with one layer. Each layer possesses distinct parameters  $\gamma$  and  $\beta$  that are tuned by an outer-loop classical optimizer.

and operate under the assumption that these servers do not communicate, placing trust in otherwise untrusted servers.

2) *Quantum Homomorphic Encryption (QHE)*: Homomorphic encryption is a cryptographic technique that allows computations to be carried out on encrypted data, yielding an encrypted result that, when decrypted, matches the result of operations performed on the plaintext [19], [21], [31], [41], [56], [68], [83], [91]. While it eliminates the need for the interactive computation intrinsic to BQC, fully-secure QHE, as suggested by the “no-go theorem,” introduces exponential computational overhead, making QHE impractical in the near term, as noisy quantum devices cannot accommodate such excessive noise accumulation. Moreover, most homomorphic encryption schemes are tailored for classical binary data, making the adaptation to quantum information—a realm governed by superposition and entanglement—particularly challenging.

3) *Hardware Architecture for Trusted Quantum Execution*: Trochatos et al. [87] recently proposed a novel hardware architecture for a trusted execution environment tailored for superconducting QCs. On the client side, post-compiling, random decoy gates/pulses are injected to obfuscate users’ circuits. On the server side, these decoy gates are attenuated inside the delusion refrigerator before executing the circuit. Assuming the delusion refrigerator functions as a trusted environment, inaccessible to the quantum server, this architecture can safeguard the security and privacy of quantum users.

However, this method comes with its own set of limitations. The technique is specific to superconducting QCs, as other QC types do not incorporate a delusion refrigerator. Additionally, the approach assumes that the quantum provider cannot access the trusted region within its own refrigerator, confining the architecture’s applicability to servers deemed trustworthy.

Moreover, QAOA circuits possess a well-defined structure, potentially enabling adversaries to discern the decoy gates. For instance, as depicted in Fig. 2(b), every edge in the problem graph corresponds to one  $R_z$  rotation, encased by two two-qubit CNOT operations. This recurring, known as an ansatz, pervades the circuit, with all instances of an ansatz in a single layer sharing the same  $\gamma$  and  $\beta$  values. It is crucial to highlight that the adversary’s aim is not the acquisition of the rotation values; rather, the goal is to retrieve the problem coefficients.

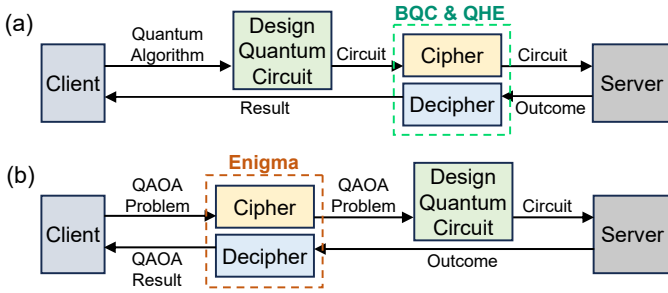


Fig. 3. Comparison of the operational area differences between prior work (a) and Enigma (b).

#### D. Goal of this Paper

Previous techniques aim to protect arbitrary quantum programs, necessitating obfuscations after the generation or compilation of quantum circuits, as shown in Figure 3(a). This required dependence on emerging technologies such as quantum networks, which are not readily available. In this paper, our goal is to concentrate on a specific application rather than developing generic SQC protocols, striking a balance between the scope of an application and its readiness for use. To that end, we propose Enigma, privacy-preserving suite of solutions specific to QAOA, as shown in Figure 3(b).

In QAOA, the problem graph embodies the proprietary data and intellectual property. Specifically, there are three attributes: coefficients, nodes, and edges. A privacy-preserving QAOA scheme must protect one or more of these attributes.

We can view QAOA from two perspectives: (a) a linear algebra problem, involving finding the eigenstate associated with the minimum eigenvalue of a given Hamiltonian matrix [10], [12]; and (b) a graph theory problem, focusing on partitioning graph nodes via edge cutting to maximize the total weight of severed edges [37], [48]. To develop our privacy-preserving technique for QAOA, we alternate between these two problem formulations and explore opportunities at their intersection.

### III. METHODOLOGY

#### A. Threat Model

**Entities:** We consider two entities: the client, who aims to solve a QAOA problem, and the server, which provides cloud access to one or multiple quantum computing devices. In our threat model, we do not distinguish between quantum computer manufacturers (e.g., IBM) and third-party cloud service providers (e.g., Amazon).

**Assets:** All information related to the QAOA problem is considered sensitive, including the number of variables, problem coefficients, and the structure of the problem graph.

**Adversaries:** We consider a malicious server (i.e., the cloud provider is malicious) or a compromised server (where a malicious insider has access). In both scenarios, we assume that the server does not tamper with the output (such tampering can be detected by checking the quality of the solution).

**Capabilities:** We assume the server can distinguish QAOA circuits and, given their structured nature, could potentially reverse-engineer them to infer the problem graph.

**Mitigations:** We propose three SQC schemes that obfuscate the QAOA problems prior to circuit creation. Each technique is designed to conceal some or all of the sensitive elements in QAOA, ranging from obscuring coefficients to introducing decoy variables and masking the problem structure.

**Residual Risk:** While we protect different attributes (coefficient, nodes, edges) by transforming the given graph, there is still some information visible to the server. For example, the transformed graph will have at-least as many nodes and edges in the problem graph as we cannot reduce the problem size.

#### B. Figure of Merit

We assess classical optimizer performance in QAOA parameter tuning using the Approximation Ratio (AR), as

$$AR = \frac{\text{Expected Value}}{\text{Global Minimum}}. \quad (2)$$

With benchmarks having negative global minima,  $AR \in (-\infty, 1]$ , where higher is better. While previous studies used AR or Approximation Ratio Gap (ARG) for comparison on the same problem [1], [6], [29], [50], [84], Enigma's problem transformation necessitates a different metric. We define the Restricted Approximation Ratio (RAR) as

$$RAR = \frac{\text{EV for the top } k \text{ outcomes}}{\text{Global Minimum}}. \quad (3)$$

Similar to AR,  $RAR \in (-\infty, 1]$ , and higher is better. In this study, we set  $k = 5$ .

To assess the obfuscation efficacy, we conduct analytical studies aimed at quantifying the difficulty an adversary would encounter when attempting to penetrate the system.

#### C. Benchmarking

We test Enigma on graphs with diverse structures: 3-regular, Sherrington–Kirkpatrick (SK) [78] (fully connected), random or Erdős–Rényi (ER) [36], [46] with edge probability 0.6, and Barabasi–Albert (BA) [14] with attachment factors of  $BA_1 = 1$  and 2, denoted by BA-1 and BA-2, respectively. Such structures benchmark QAOA performance with edge weights ( $J_{ij}$ ) from  $\{-1, +1\}$  and linear coefficients ( $h_i$ ) at zero [2], [6], [8], [17], [26], [28], [49], [54], [82], [84]. Although current quantum computers feature hundreds of qubits, their noise levels restrict reliable QAOA circuit execution to a few dozen qubits. Hence, our study's randomly generated benchmarks are limited to fewer than ten qubits, considering that embedding decoy qubits in Enigma expands the problem size.

#### D. Software and Hardware Platforms

We used the 127-qubit IBM Brisbane and IBM's Qiskit as our hardware and software platforms, respectively. Circuits are compiled at optimization level three, and executed for 10,000 trials in a noise-free (ideal simulator) and for 40,000 trials in a noisy (real) settings. For circuit parameter optimization, we utilize the COBYLA optimizer [71].

#### IV. ENIGMA-I: CIPHERING COEFFICIENTS

We present *Enigma-I*, an application-specific SQC scheme for safeguarding the security and privacy of QAOA applications by encrypting the coefficients of Ising Hamiltonians, thereby perturbing the output distribution. This renders both the input problem and the outcomes incomprehensible to compromised and malicious servers.

##### A. Overview of *Enigma-I*

*Enigma-I* leverages the property of spin variables  $\mathbf{z}$  that take values from  $\{-1, +1\}$ , where flipping the sign functions as a bit-flip in the binary domain. For a given QAOA problem, *Enigma-I* randomly selects a subset of qubits, toggles the sign of their coefficients (i.e., from  $-1 \rightarrow +1$  and vice versa), and then multiplies all coefficients by a random positive number. This effectively conceals the sign and magnitude of the problem's coefficients. Consequently, this action inverts the measurement outcomes of the targeted qubits, and only the client, who knows the list of flipped qubits, can decipher the outcomes to retrieve the correct output distribution. Figure 4 provides an overview of the *Enigma-I* scheme.

##### B. Target Qubits: Decryption Key

*Enigma-I* begins by forming a list of *target qubits*. To compile this list, qubits are uniformly and independently selected, ensuring that the size and contents of the target qubit list vary randomly each time. This list serves as the encryption key and must be securely stored, as anyone in possession of it can decrypt the QAOA output distribution.

##### C. Spin Flips: Obfuscating Sign of Coefficients

Let  $T$  be the list of target qubits. *Enigma-I* encrypts the signs of the coefficients as:

$$\hat{\mathbf{h}}_i = \begin{cases} -\mathbf{h}_i & i \in T, \\ \mathbf{h}_i & i \notin T; \end{cases} \quad (4)$$

and

$$\hat{J}_{ij} = \begin{cases} -J_{ij} & (i \in T \ \& \ j \notin T) \text{ or } (i \notin T \ \& \ j \in T), \\ J_{ij} & \text{otherwise.} \end{cases} \quad (5)$$

Figure 5(b) illustrates the impact of a spin flip by *Enigma-I* on a four-qubit problem graph (Fig. 5(a)) when  $T = \{z_1, z_2\}$ . Since target qubits are selected randomly and independently, this process effectively conceals the signs of the coefficients.

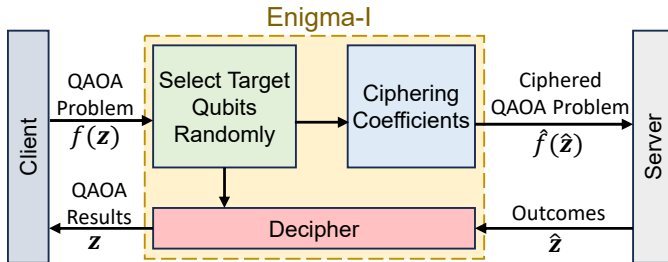


Fig. 4. Overview of *Enigma-I*

Moreover, as demonstrated in Fig. 5(b), spin flips on target qubits alter their values in the global minimum configuration without affecting the overall objective value. In essence, applying spin flips leaves the Ising Hamiltonian's energy spectrum intact but permutes the qubit states associated with each energy level. Consequently, the global minima of both the original and encrypted Hamiltonians remain the same, ensuring that while the server computes the minimum for the encrypted version, it simultaneously addresses the hidden primary problem.

##### D. Stretching: Obfuscating Magnitude of Coefficients

Multiplying any objective function  $f$  by a positive scalar  $\tau \in (0, +\infty)$  alters its scale but preserves the ordering of  $f'$ 's values. Leveraging this insight, *Enigma-I* multiplies all coefficients ( $\hat{\mathbf{h}}$  and  $\hat{J}$ ) by a randomly generated positive number  $\tau$  to obfuscate the magnitudes of the problem's coefficients.

For  $0 < \tau < 1$ ,  $f$  is contracted (Fig. 5(c)); for  $\tau > 1$ , it is stretched (Fig. 5(d)); and for  $\tau = 1$ ,  $f$  remains unchanged (Fig. 5(b)). By default, *Enigma-I* sets the value of  $\tau$  as

$$\tau = 1 + |\mathcal{N}(\mu = 1, \sigma = 1)|, \quad (6)$$

where  $\mathcal{N}(\mu = 1, \sigma = 1)$  denotes a normal random variable with mean  $\mu = 1$  and standard deviation  $\sigma = 1$ . This ensures that *Enigma-I* does not decrease the gap between the global minimum (the lowest energy level) and the first excited state (the energy level immediately above the global minimum), which is directly correlated with the success probability of quantum optimization heuristics [67].

##### E. Decrypting Outcomes

The server tunes the circuit parameters of the ciphered QAOA program, while the client is interested in the global minimum of the original QAOA problem. To retrieve the output distribution of the original problem, it is only necessary to toggle the values of the qubits in the target qubits list  $T$ , preserving their associated probability or frequency value.

##### F. Overhead of *Enigma-I*

*Enigma-I* can utilize the same parametric circuit as the primary problem, thereby imposing no additional quantum overhead. On average, *Enigma-I* takes 0.39 seconds to obfuscate problems and 0.02 seconds to decode outcomes for 500-qubit problems on a laptop, across all benchmark types. The complexity of obfuscating problems in *Enigma-I* is  $O(|J|)$ , where  $|J|$  denotes the edge count in problem graph, and the complexity of decrypting outcomes is  $O(n)$ .

##### G. Security Analysis

The list of target qubits  $T$  functions as the decryption key in *Enigma-I*, and thus, the client keeps it secret and does not share it with the server. Let  $|T|$  be the number of qubits in  $T$ , then the server would need to consider  $\binom{n}{|T|}$  possible bit flips. However, since the server is unaware of  $|T|$ , the attack complexity from an honest-but-curious server's perspective is:

$$\text{Attack Complexity} = O(2^n). \quad (7)$$

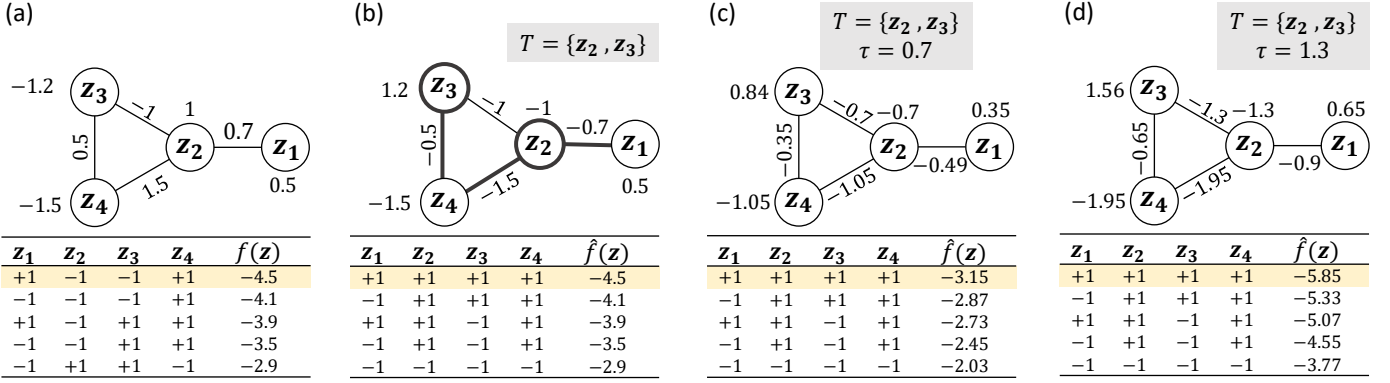


Fig. 5. A four-node QAOA problem with its cost table. The table displays the top five out of 16 arrangements, sorted with higher rows representing lower objective values, with the global minimum highlighted at the top. (a) The initial QAOA problem. (b) Result of applying spin flips to  $z_1$  and  $z_2$ . (c) Outcome of scaling all coefficients in (b) by a factor  $\tau < 1$ , which narrows the gap between energy levels. (d) Effect of scaling all coefficients in (b) by a factor  $\tau > 1$ , widening the gap between energy levels.

Enigma-I modifies the problem Hamiltonian by scaling all coefficients. However, the attacker does not need to recover the coefficients with full precision. Given Eq. (6), most  $\tau$  values fall within the range  $[1, 4]$ . Therefore, the complexity of retrieving problem coefficients with a precision of  $\alpha$  is  $\frac{1}{3\alpha}$ . For instance,  $\alpha = 1\%$  precision yields 300 combinations.

#### H. Inherent Limitation of Enigma-I

To solve a problem using QAOA, the problem must first be cast into an Ising Hamiltonian, with the Ising model's coefficients ( $\mathbf{h}$  and  $J$ ) defined so that the Ising model's global minimum corresponds to the problem's solution. Casting is tailored to each specific problem, necessitating the design of a unique casting algorithm for each application. If a particular casting algorithm invariably results in all positive (or all negative) linear coefficients  $\mathbf{h}$ , and if the server knows of such an algorithm's use, this could potentially reveal the list of target qubits, thereby decrypting the outcome bitstrings. Nonetheless, we do not currently know of any such casting algorithms, nor whether it is feasible for an algorithm to consistently produce all positive (or all negative) coefficients. It is important to note that casting algorithms may yield all zero linear coefficients ( $\mathbf{h} = 0$ ) [59], which does not aid an attacker as no information can be gleaned from a zero vector.

#### I. Evaluation Results: Proof-of-Concept

1) *Impact on Circuit Properties:* Enigma-I implements all changes directly on the coefficients of the problem Hamiltonian, and since these coefficients serve as rotation values in QAOA circuits—alongside QAOA parameters—both the baseline and Enigma-I can utilize the same parametric circuit, ensuring that Enigma-I has no effect on the circuit's properties.

2) *Impact on QAOA Fidelity:* Figure 6(a) displays the Approximation Ratio (AR) convergence for Enigma-I and standard QAOA (Baseline) on a BA-2 benchmark problem. We observed instances where Enigma-I achieved a higher AR value after tuning circuit parameters. However, since Enigma-I encrypts the QAOA problem, it results in different

optimization landscapes for the classical optimizer compared to standard QAOA circuits. Our goal is not to compare their convergence directly; rather, we aim to ensure proper convergence for both techniques.

Figure 6(b) illustrates the average Restricted Approximation Ratio (RAR) across five problem types compared to the baseline, revealing that Enigma-I lowers QAOA fidelity by up to 1% (avg. 0.7%). Enigma-I can employ the same parametric circuit as standard QAOA since all its encryptions are applied directly to problem coefficients, which are utilized as rotation values in the circuit. Therefore, any differences in fidelity between Enigma-I and the baseline, as shown in Fig. 6(b), can be attributed to the stochastic nature of quantum hardware. Consequently, Enigma-I can perform comparably to QAOA in practical applications on near-term quantum devices.

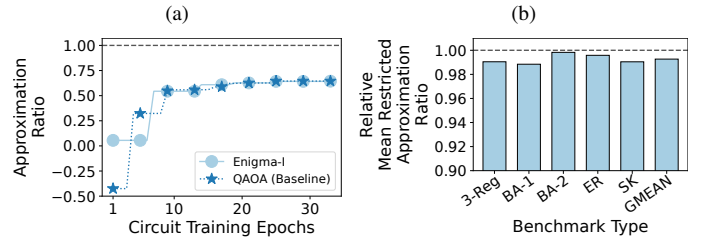


Fig. 6. (a) Approximation Ratio (AR) convergence for a BA-2 benchmark graph under noisy conditions (higher is better). (b) Mean Restricted Approximation Ratio (RAR) across various problem sizes compared to the baseline (lower is better).

#### J. Mitigations and Residual Risks

Enigma-I masks the values of QAOA coefficients and induces random spin flips on the results, effectively hiding both inputs and outputs from the server. However, the server can still access additional information, such as the qubit count, the problem graph topology, and the distribution of coefficient values. In the following section, we introduce *Enigma-II*, which offers further mitigations and reduces the residual risk.

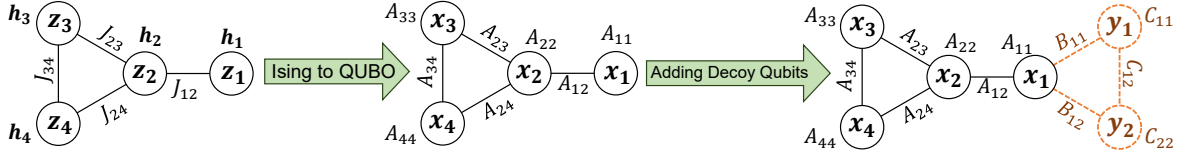


Fig. 7. Mapping the Ising model (acting on spin variables  $\mathbf{z}_i \in \{-1, +1\}$ ) to its Quadratic Unconstrained Binary Optimization (QUBO) model (acting on Binary variables  $\mathbf{x}_i \in \{0, 1\}$ ) enables Enigma-II to embed decoy qubits  $\mathbf{y}_1$  and  $\mathbf{y}_2$ , rendering them undetectable to the server. The mapping involves calculating QUBO coefficients (linear:  $A_{ii}$ ; quadratic:  $A_{ij}$ ) from the Ising model's coefficients (linear:  $\mathbf{h}$ ; quadratic:  $J$ ). In the obfuscated problem,  $B$  and  $C$  represent the coefficients for decoy terms.

## V. ENIGMA-II: ADDING DECOY QUBITS

We introduce *Enigma-II*, an enhancement of Enigma-I, which obfuscates the problem structure by embedding decoy qubits indetectable to the server, thereby offering advanced protection for QAOA users. However, integrating decoy qubits with existing qubits is nontrivial. It is essential for clients to correctly interpret the solution of the original problem from the obfuscated solution provided by the server. The Ising model, which uses spin variables  $\mathbf{z}_i \in \{-1, +1\}$ , can be transformed into the Quadratic Unconstrained Binary Optimization (QUBO) model, where the variables are binary  $\mathbf{x}_i \in \{0, 1\}$ . This transformation is important because it allows us to apply linear algebra techniques. By converting the Ising model to a QUBO model, we can express the objective function in a matrix form [10], [12]. This matrix representation is helpful in using linear algebra methods to accurately recover the solution, as illustrated in Fig. 7. Figure 8 illustrates the process of mapping between Ising and QUBO models.

### A. Overview of Enigma-II

Figure 9 overviews the Enigma-II scheme. It transforms the Ising Hamiltonian to QUBO, introduces decoy variables, and permutes them to obscure primary and decoy variables. After reverting to the Ising model, it applies a final obfuscation with Enigma-I before server submission.

### B. Transforming Ising to QUBO: Facilitating Matrix Representation for Solution Recovery

Enigma-II begins by transforming the input Ising Hamiltonian into a QUBO formulation:  $f(\mathbf{z}) \mapsto g(\mathbf{x})$  (Fig. 7). Given  $\mathbf{x}_i \in \{0, 1\}$ , the task of finding the global minimum of  $g(\mathbf{x})$  is equivalent to minimizing

$$\mathbf{x}^T \mathbf{A} \mathbf{x}, \quad (8)$$

$$\begin{aligned}
 f(\mathbf{z}) &= \sum_i \mathbf{h}_i \mathbf{z}_i + \sum_{i < j} J_{ij} \mathbf{z}_i \mathbf{z}_j + c_{\text{Ising}} \\
 A_{ii} &= 2(\mathbf{h}_i - \sum_j J_{ij} + \sum_j J_{ji})_i \\
 A_{ij} &= 4J_{ij}, \quad i \neq j \\
 c_{\text{QUBO}} &= c_{\text{Ising}} + \sum_{i \neq j} J_{ij} - \sum_i \mathbf{h}_i \\
 g(\mathbf{x}) &= \sum_i A_{ii} \mathbf{x}_i + \sum_{i < j} A_{ij} \mathbf{x}_i \mathbf{x}_j + c_{\text{QUBO}}
 \end{aligned}
 \quad
 \begin{aligned}
 \mathbf{h}_i &= \frac{A_{ii}}{2} + \frac{\sum_j A_{ij} + \sum_j A_{ji}}{4} \\
 J_{ij} &= \frac{A_{ij}}{4}, \quad i \neq j \\
 c_{\text{Ising}} &= c_{\text{QUBO}} + \frac{\sum_i A_{ii}}{2} + \frac{\sum_{i \neq j} A_{ij}}{4}
 \end{aligned}$$

Fig. 8. Linear Transformability of the Ising Hamiltonian— $f(\mathbf{z})$  with  $\mathbf{z}_i \in \{-1, +1\}$ —and the Quadratic Unconstrained Binary Optimization (QUBO)— $g(\mathbf{x})$  with  $\mathbf{x}_i \in \{0, 1\}$ , depicting the linear conversion process between the two representations.

where  $A$  is the coefficient matrix with its diagonal elements,  $A_{ii}$ , representing linear coefficients and off-diagonal elements representing quadratic coefficients.

### C. Embedding Decoy Qubits

Enigma-II perturbs problem structure by appending  $m$  decoy variables, denoted by  $\mathbf{y}$  to the  $\mathbf{x}$  as:

$$\tilde{\mathbf{x}} = [\mathbf{x}_1, \mathbf{x}_2, \dots, \mathbf{x}_n, \mathbf{y}_1, \mathbf{y}_2, \dots, \mathbf{y}_m]^T \quad (9)$$

However, simply adding decoy variables is insufficient; they must be indistinguishable to the server by creating decoy quadratic terms. To this end, the coefficient matrix  $A$  is augmented to

$$\tilde{A} = \begin{pmatrix} A & B \\ B^T & C \end{pmatrix}, \quad (10)$$

Where  $B \in \mathbb{R}^{n \times m}$  is the interaction matrix between  $\mathbf{x}$  and  $\mathbf{y}$ , and  $C \in \mathbb{R}^{m \times m}$  for  $\mathbf{y}$  interactions (Fig. 7). Hence, minimizing (8) is recast as minimizing

$$\tilde{\mathbf{x}}^T \tilde{A} \tilde{\mathbf{x}}. \quad (11)$$

### D. Guarantying a Successful Recovery

The global minimum of the original problem—concealed from the server—must be recoverable using the solution to the obfuscated problem provided by the server. Let  $\mathbf{x}^*$  and  $\tilde{\mathbf{x}}^*$  represent the global minima of (8) and (11), respectively. Enigma-II ensures that  $\mathbf{x}^*$  and  $\tilde{\mathbf{x}}^*$  consistently match in primary variable values through constraints on  $B$  and  $C$ . Note that the value of decoy variables ( $\mathbf{y}$ ) is immaterial.

Expanding (11) follows

$$\begin{aligned}
 \tilde{\mathbf{x}}^T \tilde{A} \tilde{\mathbf{x}} &= \begin{pmatrix} \mathbf{x}^T & \mathbf{y}^T \end{pmatrix} \begin{pmatrix} A & B \\ B^T & C \end{pmatrix} \begin{pmatrix} \mathbf{x} \\ \mathbf{y} \end{pmatrix} \\
 &= \mathbf{x}^T \mathbf{A} \mathbf{x} + 2\mathbf{x}^T \mathbf{B} \mathbf{y} + \mathbf{y}^T \mathbf{C} \mathbf{y}. \quad (12)
 \end{aligned}$$

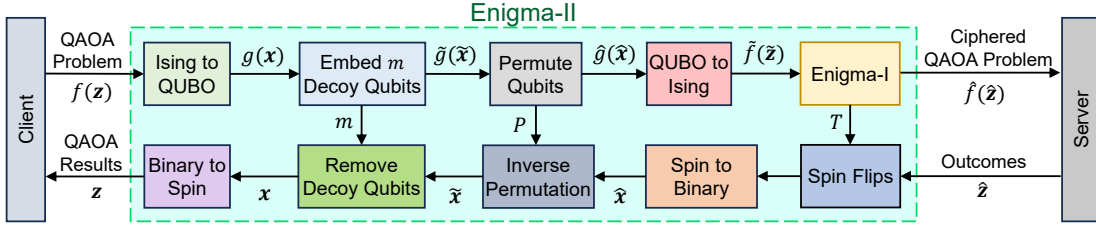


Fig. 9. Overview of Enigma-II

Our objective is to guarantee that

$$\tilde{\mathbf{x}}^* = [\mathbf{x}^*; \mathbf{y}^*]. \quad (13)$$

We argue that satisfying the following conditions is sufficient for 13 to hold:

- 1)  $B$  is non-negative;
- 2)  $C$  is such that  $\mathbf{y}^*$  is the global minimum of  $\mathbf{y}^T C \mathbf{y}$ ;
- 3)  $\mathbf{x}^T B \mathbf{y}^* = 0$  for any binary  $\mathbf{x}$ .

Values of  $B$  and  $C$  are drawn randomly from positive distributions (see Section V-E), thus the first constraint is readily addressed during the generation of decoy edge weights. To meet the other constraints, we define  $\mathbf{y}^*$  as the zero vector  $[0, 0, \dots, 0]^T$ . With  $\mathbf{y}_i \in \{0, 1\}$ , a non-negative matrix  $C$  ensures compliance with the second and third constraints.

#### E. Adding Decoy Edges: Uniformizing Coefficients

Decoy edges are introduced to render the decoy variables indistinguishable to the server. There are two types of decoy edges: (a) those connecting a primary variable  $\mathbf{x}_i$  to a decoy variable  $\mathbf{y}_j$ , established by assigning a nonzero positive value to  $B_{ij}$ ; and (b) those between two decoy variables  $\mathbf{y}_i$  and  $\mathbf{y}_j$ , created by setting  $C_{ij}$  to a nonzero positive value. These decoy edges correspond to new (decoy) quadratic terms.

Enigma-II randomly specifies both the positions and values of nonzero entries in matrices  $B$  and  $C$ . For each column of  $B$ , Enigma-II generates a random integer  $k_i^{\text{out}}$  within the range of one to  $k_{\text{max}}^{\text{out}}$  (default:  $k_{\text{max}}^{\text{out}} = 1$ ), and randomly selects  $k_i^{\text{out}}$  rows in that column to assign nonzero positive values. Likewise, each column of  $C$  is assigned at least one and no more than  $k_{\text{max}}^{\text{in}}$  nonzero entries (default:  $k_{\text{max}}^{\text{in}} = 1$ ).

Inspired by the natural selection operator in evolutionary algorithms [33], [57], [77], [80], Enigma-II employs a roulette wheel to generate random weights for decoy edges. Existing coefficients are bucketed into  $b$  bins (default:  $b = 10$ ), and normalized frequency values serve as the probability of the associated bins, denoted by  $p_i$ . To construct the roulette wheel, Enigma-II offers two options for defining the sector values  $R_i$  associated with  $b_i$ : (a)  $R_i = p_i$ , preserving the distribution of existing coefficients; and (b)  $R_i = \frac{1}{p_i}$  (i.e., using inverse probability), uniformizing the final coefficient distribution (see Fig. 10). By default, Enigma-II opts for the latter to obscure the coefficient magnitude distribution from the server. All decoy edge weights are positive (see Section V-D); however, Enigma-II takes additional measures (see Section V-G) to conceal the distribution of coefficient signs.

#### F. Permuting Qubits

Appending decoy variables to the end (or beginning) of the vector of primary variables (i.e.,  $\tilde{\mathbf{x}} = [\mathbf{x}, \mathbf{y}]$ ) may make most—but not all—decoy qubits distinguishable to the server. It is important to note that the number of decoy variables,  $m$ , remains concealed from the server. To ensure that primary and decoy variables are indistinguishable from each other, Enigma-II permutes the entries of  $\tilde{\mathbf{x}}$ .

Enigma-II generates a random permutation matrix  $P \in \{0, 1\}^{(N+m) \times (N+m)}$ . A permutation matrix is a sparse matrix with exactly one nonzero entry in each row and column, and since  $\tilde{\mathbf{x}}$  is a binary vector, all nonzero entries of  $P$  are ones. Shuffling the columns of the identity matrix  $I$  produces a random permutation matrix.

Since  $P$  is a unitary matrix, we have  $P^{-1} = P^T$ . Therefore, we can rewrite (11) as

$$\begin{aligned} \tilde{\mathbf{x}}^T \tilde{A} \tilde{\mathbf{x}} &= \tilde{\mathbf{x}}^T P^T P \tilde{A} P^T P \tilde{\mathbf{x}} \\ &= (\tilde{\mathbf{x}}^T P^T) (P \tilde{A} P^T) (P \tilde{\mathbf{x}}) \\ &= \hat{\mathbf{x}}^T \hat{A} \hat{\mathbf{x}}, \end{aligned} \quad (14)$$

where  $\hat{\mathbf{x}} = P \tilde{\mathbf{x}}$  and  $\hat{A} = P \tilde{A} P^T$ . In the reformulated scenario, only the coefficient matrix  $\hat{A}$  of the obscured problem is disclosed to the server.

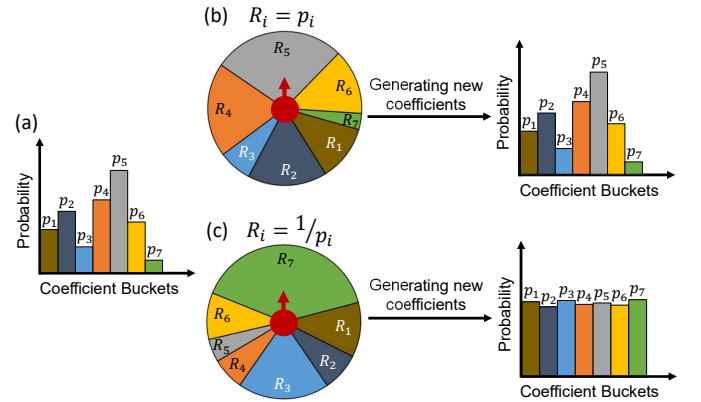


Fig. 10. (a) The distribution of problem coefficient values. (b) Generating decoy edge weights using the current probability distribution preserves its profile. (c) Employing inverse probability in the roulette wheel approach yields a more uniform coefficient distribution.



### G. Forming Ising Hamiltonian

Both Ising and QUBO models are linearly equivalent, as shown in Fig. 8. However, Enigma-II transforms  $\hat{A}$  into an Ising Hamiltonian and applies Enigma-I for additional obfuscation before sharing  $\hat{\mathbf{h}}$  and  $\hat{\mathbf{J}}$  with the server.

### H. Decrypting Outcomes

Decrypting outcomes with Enigma-II follows the reverse sequence of the obfuscation layers applied. Initially, the decryption is facilitated by Enigma-I’s decryption module using the *target qubits* list ( $T$ ), which then remaps the resulting spin variables into the binary domain, yielding  $\hat{\mathbf{x}}$ . The permutation’s effect is subsequently undone by

$$\tilde{\mathbf{x}} = P^T \hat{\mathbf{x}} = [\mathbf{x}_1^*, \mathbf{x}_2^*, \dots, \mathbf{x}_n^*, \mathbf{y}_1^*, \mathbf{y}_2^*, \dots, \mathbf{y}_m^*]^T. \quad (15)$$

Here, the primary variables  $\mathbf{x}$  are represented by the first  $n$  elements, while the final  $m$  elements—associated with the decoy variables—are omitted, as they hold no value for the client. Notably, the knowledge of the exact count of decoy variables  $m$  is exclusive to the client.

### I. Overhead of Enigma-II

The primary quantum overhead for Enigma-II is adding  $m$  decoy qubits, where  $m$  is user-defined and remains constant regardless of the problem size. On average, Enigma-II requires 6.53 seconds to obfuscate and 1.04 seconds to decode outcomes for 500-qubit problems on a standard laptop, across all benchmark types. The computational complexities for the obfuscation and decoding processes in Enigma-II are  $O((n+m)^3)$  and  $O((n+m)^2)$ , respectively.

### J. Security Analysis

Decrypting Enigma-II outcomes includes three layers: (a) attenuating spin flips caused by Enigma-I (the last step of Enigma-II), with the attack complexity of  $2^{n+m}$ ; (b) undoing the variable permutation, examining  $(n+m)!$  possible permutation matrices; and (c) extracting  $n$  primary variables from a vector of size  $n+m$ , with the complexity of  $n+m$  as the attacker is unaware of  $m$  and whether decoy variables have been added to the beginning or end of the primary variable vector. Hence, the attack complexity in Enigma-II from an honest-but-curious server’s perspective is:

$$\text{Attack Complexity} = O((n+m) \times (n+m)! \times 2^{n+m}). \quad (16)$$

### K. Inherent Limitation of Enigma-II

When a problem graph is regular, embedding decoy qubits randomly can aid an attacker in identifying them, as they deviate from the general graph structure. As  $m \rightarrow \infty$ , the output graph theoretically becomes random, but this is impractical since each decoy variable requires one qubit. Therefore, for regular graphs, Enigma-II is not advisable; instead, users should opt for Enigma-I or Enigma-III (Section VI). In the case of fully connected graphs, however, connecting decoy qubits to all existing qubits preserves the fully-connected structure in the obfuscated graph.

### L. Evaluation Results: Proof-of-Concept

1) *Impact on Circuit Properties:* Figure 11(a) shows the GMEAN of IBM’s native two-qubit gate (ECR) count for Enigma-II with one and two decoy qubits ( $m = 1$  and 2), relative to the baseline, across all benchmark types. We observe that since  $m$  does not scale with  $n$ , the relative impact of embedding decoy qubits decreases as the problem size increases ( $m/n \rightarrow 0$  as  $n \rightarrow \infty$ ). Similarly, Fig. 11(b) shows the circuit depth for Enigma-II with  $m = 1$  and 2 across five benchmark types in comparison to standard QAOA. The fluctuations depicted in Fig. 11(b) are due to the stochastic nature of the compilation techniques, and we generally expect similar trends in circuit depth and ECR count.

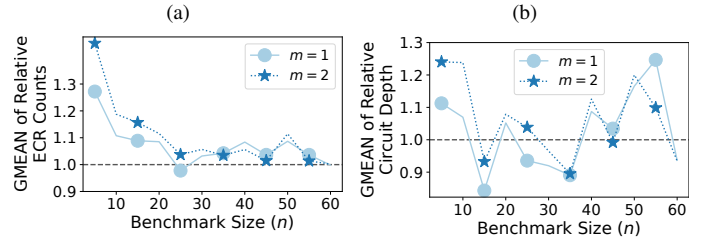


Fig. 11. GMEAN of ENIGMA-II’s circuit properties (embedding  $m = 1$  and 2 decoy qubits), relative to the standard QAOA Circuit (baseline), post-compiling for IBM Brisbane, across five benchmark graph types: (a) Echoed Cross-Resonance (ECR) gate counts, and (b) circuit depth. Lower is better.

2) *Impact on Fidelity:* Figure 12(a) shows the AR convergence for Enigma-II and standard QAOA on a BA-2 benchmark problem. Note that as Enigma-II encrypts the QAOA problem, it and the baseline address distinct problems with different QAOA circuit landscapes. Figure 12(b) depicts the average RAR across five problem types relative to the baseline, where Enigma-II is observed to reduce QAOA fidelity by up to 4% (avg. 2%) with the embedding of  $m = 1$  decoy qubit.

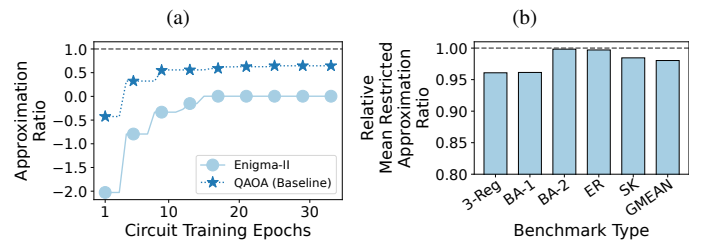


Fig. 12. (a) AR convergence for a BA-2 benchmark graph under noisy conditions (higher is better). (b) Mean RAR across various problem sizes compared to the baseline (lower is better).

### M. Mitigations and Residual Risks

Enigma-II can obscure most aspects of QAOA information; however, certain sources of information, such as the overall structure of the problem graph, remain visible to the server. For instance, in problems involving “power-law” graph structures, merely adding decoy gates does not conceal the hotspots [6]. In the following section, we introduce *Enigma-III*, which offers further mitigations and reduces the residual risk.

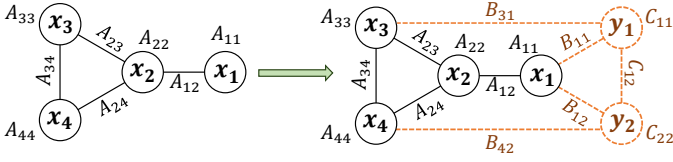


Fig. 13. Enigma-III embeds two decoy variables ( $y_1$  and  $y_2$ ) to transform the input Dragon graph into a 3-regular graph.

## VI. ENIGMA-III: REGULARIZING QUBITS

We present *Enigma-III*, which strategically incorporates decoy qubits to regularize the problem graph, effectively concealing its structure from the server as demonstrated in Fig. 13. Paul Erdős (1963) proved that regularizing any graph is possible through the addition of new nodes and the meticulous placement of edges: new nodes are connected to existing ones and to each other without adding links between the original nodes [35]. Utilizing this insight, Enigma-III calculates the least number of decoy qubits needed to regularize the input problem and strategically introduces decoy edges to equalize the degree across all qubits.

### A. Enigma-II vs. Enigma-III

Enigma-III differs from Enigma-II in two key aspects: (a) Unlike Enigma-II, where the client sets the number of decoy variables  $m$ , Enigma-III algorithmically determines  $m$  to achieve a regular graph structure; and (b) the introduction of decoy edges is not random but rather orchestrated to ensure that all variables, including both primary and decoy, have the same degree (Fig. 13).

### B. How Many Decoy Qubits?

Let  $d_i$  be the degree of  $x_i$ , and let  $d^*$  (where  $d^* \geq d_i$  for all  $i$ ) be the target degree for the regular graph's output. The deficiency of  $x_i$  is defined as

$$e_i = d^* - d_i, \quad (17)$$

and the total deficiency of the problem graph is

$$s = \sum_{i=1}^n e_i. \quad (18)$$

Let  $m$  be the number of decoy variables. Meeting the following conditions is necessary and sufficient for rendering the graph  $d^*$ -regular [35]:

- 1)  $md^* \geq s$ ;
- 2)  $m^2 - (d^* + 1)m + s \geq 0$ ;
- 3)  $m \geq \max(e_i)$ ;
- 4)  $(m + n)d^*$  is an even number.

Introducing each decoy variable requires an additional qubit; therefore, we seek the smallest integer  $m$  that satisfies all four aforementioned conditions. We observe that Solvers like Z3 [9], [30] may be unsuitable for large-scale problems due to potential computational delays in determining the minimal  $m$ . However, as  $m = O(n)$ , we observe that a linear search from  $m_{\min}$  (default:  $m_{\min} = 0$ ) to  $n$  can efficiently solve this problem, often in less than a second.

### C. How to Add Decoy Qubits?

After determining  $m$ , Enigma-III first ensures that the primary variables attain a degree of  $d^*$  by establishing connections between decoy and primary nodes. Subsequently, it connects decoy nodes with degrees less than  $d^*$ , prioritizing those with the highest deficiency, until all  $n + m$  nodes reach a degree of  $d^*$ , thus forming a  $d^*$ -regular graph.

### D. Overhead of Enigma-III

The primary quantum overhead of Enigma-III is adding  $m$  decoy qubits; however, unlike Enigma-II,  $m$  scales sub-linearly with  $n$ . On average, Enigma-III employs 15.4 seconds to obfuscate and 1.32 seconds to decode outcomes for 500-qubit problems on a standard laptop, across all benchmark types. The computational complexity of Enigma-III is similar to that of Enigma-II.

### E. Security Analysis

While Enigma-III enhances privacy by regularizing the obfuscated problem graph, it shares the same attack complexity with Enigma-II, as detailed below:

$$\text{Attack Complexity} = O((n + m) \times (n + m)! \times 2^{n+m}). \quad (19)$$

### F. Evaluation Results: Proof-of-Concept

1) *Impact on Circuit Properties*: Figure 14(a) displays the GMEAN of IBM's native two-qubit gate (ECR) count and circuit depth for Enigma-III compared to the baseline across all benchmark types, indicating a linear scaling of ECR count and circuit depth with problem size. Likewise, Fig. 14(b) shows that the number of decoy qubits in Enigma-III increases sub-linearly with problem size.

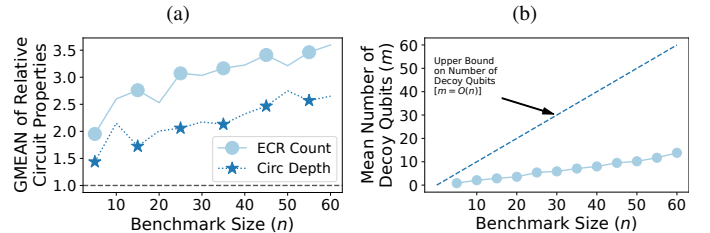


Fig. 14. (a) GMEAN of ENIGMA-III's QAOA circuit properties, relative to the standard QAOA Circuit (baseline), post-compiling for IBM Brisbane, across five benchmark graph types. (b) Mean number of decoy qubits ( $m$ ) required by Enigma-III to regularize problem graphs across five benchmark graph topologies. Lower is better.

2) *Impact on Fidelity*: Figure 15(a) illustrates the convergence of the AR for Enigma-III and standard QAOA on a BA-2 benchmark problem. Figure 15(b) presents the average RAR across various problem sizes in comparison to the baseline. We observe that regularizing the problem graphs can lower the QAOA fidelity by up to 30% (avg. 13%). As quantum hardware improves and device error reduces, a lesser reduction in fidelity by Enigma-III can be expected in the near term.

### G. Mitigations and Residual Risks

Enigma-III provides the highest level of privacy for QAOA applications. However, although the obfuscated problem graph is regularized, the degree of this regular graph serves as an upper bound for the node with the highest degree in the primary graph, information that remains visible to the server. Currently, we are unaware of any security or privacy issues associated with this piece of information.

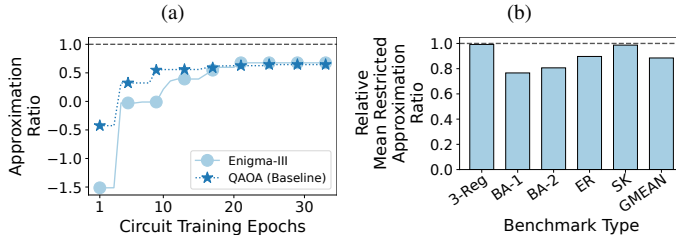


Fig. 15. (a) AR convergence for a BA-2 benchmark graph under noisy conditions (higher is better). (b) Mean RAR across various problem sizes compared to the baseline (lower is better).

### VII. WHEN AND WHERE TO USE ENIGMA?

Enigma-I conceals both problem coefficients and results without incurring additional quantum overhead, making it immediately deployable on current and near-term QCs. Enigma-I is particularly effective for regular input problems, a common characteristic in real-world scenarios. Importantly, when an attacker encounters a regular problem, it cannot discern if the problem was inherently regular or regularized by Enigma-III. Enigma-I can offer enhanced privacy without any quantum overhead or fidelity reduction.

Enigma-II builds on Enigma-I by introducing decoy qubits to perturb the problem’s structure. In Enigma-II, the number of decoy qubits  $m$  does not scale with the problem size  $n$ , which is advantageous for near-term quantum computers as the relative impact of adding decoy qubits diminishes with increasing problem size ( $m/n \rightarrow 0$  as  $n \rightarrow \infty$ ). Enigma-II is particularly suitable for problems with irregular or random structures, where it is challenging for attackers to identify decoy qubits. However, Enigma-II is not recommended for regular problem graphs, as decoy qubits can be more readily detected by an attacker.

Enigma-III provides the highest level of protection by embedding additional decoy qubits to regularize the problem. Contrary to Enigma-II, where  $m$  is independent of  $n$ , in Enigma-III,  $m$  increases sub-linearly with the problem size, making it well-suited for the forthcoming generation of quantum hardware expected to have lower device errors.

With the Ising model adopted as the standard input for emerging optimization accelerators, both quantum and classical, the scope and applicability of Enigma schemes expand beyond QAOA to include platforms such as optical Ising processors [53], [60], [70], Fujitsu’s digital annealers [3], [65], [75], Toshiba’s simulated bifurcation machines [47], [85], [86], and quantum annealers [7], [61].

### VIII. RELATED WORK

Secure Quantum Computing (SQC) is a nascent field that tackles the delegation of quantum programs to untrusted remote servers, categorizing techniques mainly into Blind Quantum Computing (BQC) and Quantum Homomorphic Encryption (QHE). Traditional BQC protocols typically presuppose quantum capabilities on the client’s side [20], [23], [42], [43], [55], [64], depending on a quantum network infrastructure that’s not yet universally accessible. Recent techniques [42], [44], [45], [51], [62], [73] allow classical clients to operate using multiple, non-communicating servers, a practice that paradoxically relies on “untrusted” entities. QHE, on the other hand, accommodates classical clients on a single server but confronts notable hurdles, such as exponential computational overheads and the prerequisite of sophisticated quantum error correction [19], [21], [31], [41], [56], [68], [83], [91]. In contrast, Enigma avoids reliance on emerging technologies or segregated servers, offering polynomial computational overhead, thereby making it a viable option for current and near-term quantum systems.

A recent study [87] proposes a quantum hardware architecture tailored for superconducting QCs. Although promising, this approach may not be secure for near-term quantum programs with well-structured circuits. On the other hand, Enigma can protect the privacy of QAOA applications across all types of quantum devices.

### IX. CONCLUSION

We propose *Enigma* as a SQC protocol specifically designed to safeguard the privacy of QAOA applications executed on untrusted quantum computers. QAOA applications comprise three types of sensitive information: coefficients, problem topology, and variable values. To address these, we introduce three distinct schemes, each targeting different QAOA aspects.

*Enigma-I* obscures the values of QAOA coefficients and triggers random spin flips in the results, effectively concealing both the inputs and outputs from the server’s perspective. However, the server might still access additional information, such as the qubit count and the problem graph’s topology. To address this, we present *Enigma-II*, which builds on Enigma-I by integrating decoy variables to disturb and mask the problem’s structure. While Enigma-II can veil most QAOA information facets, some information, like the problem graph’s general structure, can still be discerned by the server. To mitigate this, we introduce *Enigma-III*, which enhances Enigma-II by strategically embedding decoy variables so that all variables in the resulting problem have the same degree, thereby regularizing the problem graph. For all Enigma variants, we guarantee the retrieval of solutions for the original problem. Our experiments show that Enigma’s privacy enhancements incur only a minor fidelity reduction (1%–13%).

To the best of our knowledge, Enigma stands as the first application-specific SQC proposal and the first privacy-preserving framework that is immediately deployable on current and near-term QCs.

## REFERENCES

- [1] M. Alam, A. Ash-Saki, and S. Ghosh, "Circuit compilation methodologies for quantum approximate optimization algorithm," in *2020 53rd Annual IEEE/ACM International Symposium on Microarchitecture (MICRO)*. IEEE, 2020, pp. 215–228.
- [2] M. Alam, A. Ash-Saki, and S. Ghosh, "An efficient circuit compilation flow for quantum approximate optimization algorithm," in *2020 57th ACM/IEEE Design Automation Conference (DAC)*. IEEE, 2020, pp. 1–6.
- [3] M. Aramon, G. Rosenberg, E. Valiante, T. Miyazawa, H. Tamura, and H. G. Katzgraber, "Physics-inspired optimization for quadratic unconstrained problems using a digital annealer," *Frontiers in Physics*, vol. 7, p. 48, 2019.
- [4] F. Arute, K. Arya, R. Babbush, D. Bacon, J. C. Bardin, R. Barends, R. Biswas, S. Boixo, F. G. Brandao, D. A. Buell *et al.*, "Quantum supremacy using a programmable superconducting processor," *Nature*, vol. 574, no. 7779, pp. 505–510, 2019.
- [5] R. Ayanzadeh, "Leveraging artificial intelligence to advance problem-solving with quantum annealers," Ph.D. dissertation, University of Maryland, Baltimore County, 2020.
- [6] R. Ayanzadeh, N. Alavisamani, P. Das, and M. Qureshi, "Frozenqubits: Boosting fidelity of qaoa by skipping hotspot nodes," in *Proceedings of the 28th ACM International Conference on Architectural Support for Programming Languages and Operating Systems, Volume 2*, 2023, pp. 311–324.
- [7] R. Ayanzadeh, P. Das, S. Tannu, and M. Qureshi, "Equal: Improving the fidelity of quantum annealers by injecting controlled perturbations," in *2022 IEEE International Conference on Quantum Computing and Engineering (QCE)*. IEEE, 2022, pp. 516–527.
- [8] R. Ayanzadeh, J. Dorband, M. Halem, and T. Finin, "Multi-qubit correction for quantum annealers," *Scientific Reports*, vol. 11, no. 1, p. 16119, 2021.
- [9] R. Ayanzadeh, M. Halem, and T. Finin, "Sat-based compressive sensing," *arXiv preprint arXiv:1903.03650*, 2019.
- [10] R. Ayanzadeh, M. Halem, and T. Finin, "An ensemble approach for compressive sensing with quantum annealers," in *IGARSS 2020-2020 IEEE International Geoscience and Remote Sensing Symposium*. IEEE, 2020, pp. 3517–3520.
- [11] R. Ayanzadeh, M. Halem, and T. Finin, "Reinforcement quantum annealing: A hybrid quantum learning automata," *Scientific Reports*, vol. 10, no. 1, pp. 1–11, 2020.
- [12] R. Ayanzadeh, S. Mousavi, M. Halem, and T. Finin, "Quantum annealing based binary compressive sensing with matrix uncertainty," *arXiv preprint arXiv:1901.00088*, 2019.
- [13] J. S. Baker and S. K. Radha, "Wasserstein solution quality and the quantum approximate optimization algorithm: A portfolio optimization case study," *arXiv preprint arXiv:2202.06782*, 2022.
- [14] A.-L. Barabási, R. Albert, and H. Jeong, "Scale-free characteristics of random networks: the topology of the world-wide web," *Physica A: statistical mechanics and its applications*, vol. 281, no. 1-4, pp. 69–77, 2000.
- [15] P. K. Barkoutsos, G. Nannicini, A. Robert, I. Tavernelli, and S. Woerner, "Improving variational quantum optimization using CVaR," *Quantum*, vol. 4, p. 256, apr 2020. [Online]. Available: <https://doi.org/10.22331/q-2020-04-20-256>
- [16] S. Barz, E. Kashefi, A. Broadbent, J. F. Fitzsimons, A. Zeilinger, and P. Walther, "Demonstration of blind quantum computing," *science*, vol. 335, no. 6066, pp. 303–308, 2012.
- [17] J. Basso, E. Farhi, K. Marwaha, B. Villalonga, and L. Zhou, "The quantum approximate optimization algorithm at high depth for maxcut on large-girth regular graphs and the sherrington-kirkpatrick model," *arXiv preprint arXiv:2110.14206*, 2021.
- [18] S. Brandhofer, D. Braun, V. Dehn, G. Hellstern, M. Hüls, Y. Ji, I. Polian, A. S. Bhatia, and T. Wellens, "Benchmarking the performance of portfolio optimization with qaoa," 2022. [Online]. Available: <https://arxiv.org/abs/2207.10555>
- [19] A. Broadbent, "Delegating private quantum computations," *Canadian Journal of Physics*, vol. 93, no. 9, pp. 941–946, 2015.
- [20] A. Broadbent, J. Fitzsimons, and E. Kashefi, "Universal blind quantum computation," in *2009 50th annual IEEE symposium on foundations of computer science*. IEEE, 2009, pp. 517–526.
- [21] A. Broadbent and S. Jeffery, "Quantum homomorphic encryption for circuits of low t-gate complexity," in *Annual Cryptology Conference*. Springer, 2015, pp. 609–629.
- [22] O. Bulancea Lindvall, "Quantum methods for sequence alignment and metagenomics," 2019.
- [23] A. M. Childs, "Secure assisted quantum computation," *arXiv preprint quant-ph/0111046*, 2001.
- [24] J. Choi, S. Oh, and J. Kim, "Quantum approximation for wireless scheduling," *Applied Sciences*, vol. 10, no. 20, p. 7116, 2020.
- [25] B. A. Cordier, N. P. Sawaya, G. G. Guerreschi, and S. K. McWeeney, "Biology and medicine in the landscape of quantum advantages," *arXiv preprint arXiv:2112.00760*, 2021.
- [26] G. E. Crooks, "Performance of the quantum approximate optimization algorithm on the maximum cut problem," *arXiv preprint arXiv:1811.08419*, 2018.
- [27] C. Dalyac, L. Henriet, E. Jeandel, W. Lechner, S. Perdrix, M. Porcheron, and M. Veshchezerova, "Qualifying quantum approaches for hard industrial optimization problems. a case study in the field of smart-charging of electric vehicles," *EPJ Quantum Technology*, vol. 8, no. 1, p. 12, 2021.
- [28] A. Das and B. K. Chakrabarti, "Colloquium: Quantum annealing and analog quantum computation," *Reviews of Modern Physics*, vol. 80, no. 3, p. 1061, 2008.
- [29] P. Das, S. Tannu, and M. Qureshi, "Jigsaw: Boosting fidelity of nisq programs via measurement subsetting," in *MICRO-54*, 2021, pp. 937–949. [Online]. Available: <https://dl.acm.org/doi/pdf/10.1145/3466752.3480044>
- [30] L. De Moura and N. Bjørner, "Z3: An efficient smt solver," in *International conference on Tools and Algorithms for the Construction and Analysis of Systems*. Springer, 2008, pp. 337–340.
- [31] Y. Dulek, C. Schaffner, and F. Speelman, "Quantum homomorphic encryption for polynomial-sized circuits," in *Advances in Cryptology—CRYPTO 2016: 36th Annual International Cryptology Conference, Santa Barbara, CA, USA, August 14–18, 2016, Proceedings, Part III 36*. Springer, 2016, pp. 3–32.
- [32] D. J. Egger, C. Gambella, J. Marecek, S. McFaddin, M. Mevissen, R. Raymond, A. Simonetto, S. Woerner, and E. Yndurain, "Quantum computing for finance: State-of-the-art and future prospects," *IEEE Transactions on Quantum Engineering*, vol. 1, pp. 1–24, 2020.
- [33] A. E. Eiben and J. E. Smith, *Introduction to evolutionary computing*. Springer, 2015.
- [34] P. S. Emani, J. Warrell, A. Anticevic, S. Bekiranov, M. Gandal, M. J. McConnell, G. Sapiro, A. Aspuru-Guzik, J. T. Baker, M. Bastiani *et al.*, "Quantum computing at the frontiers of biological sciences," *Nature Methods*, vol. 18, no. 7, pp. 701–709, 2021.
- [35] P. Erdős and P. Kelly, "The minimal regular graph containing a given graph," *Amer. Math. Monthly*, vol. 70, pp. 1074–1075, 1963.
- [36] P. Erdős, A. Rényi *et al.*, "On the evolution of random graphs," *Publ. math. inst. hung. acad. sci.*, vol. 5, no. 1, pp. 17–60, 1960.
- [37] E. Farhi, J. Goldstone, and S. Gutmann, "A quantum approximate optimization algorithm," *arXiv preprint arXiv:1411.4028*, 2014.
- [38] E. Farhi, J. Goldstone, and S. Gutmann, "A quantum approximate optimization algorithm applied to a bounded occurrence constraint problem," *arXiv preprint arXiv:1412.6062*, 2014.
- [39] R. Feynman, "Simulating physics with computers," *International Journal of Theoretical Physics*, vol. 21, no. 6, 1982.
- [40] M. Fingerhuth, T. Babej, and C. Ing, "A quantum alternating operator ansatz with hard and soft constraints for lattice protein folding," 2018. [Online]. Available: <https://arxiv.org/abs/1810.13411>
- [41] K. A. Fisher, A. Broadbent, L. Shalm, Z. Yan, J. Lavoie, R. Prevedel, T. Jennewein, and K. J. Resch, "Quantum computing on encrypted data," *Nature communications*, vol. 5, no. 1, p. 3074, 2014.
- [42] J. F. Fitzsimons, "Private quantum computation: an introduction to blind quantum computing and related protocols," *npj Quantum Information*, vol. 3, no. 1, p. 23, 2017.
- [43] J. F. Fitzsimons and E. Kashefi, "Unconditionally verifiable blind quantum computation," *Physical Review A*, vol. 96, no. 1, p. 012303, 2017.
- [44] A. Gheorghiu, E. Kashefi, and P. Wallden, "Robustness and device independence of verifiable blind quantum computing," *New Journal of Physics*, vol. 17, no. 8, p. 083040, 2015.
- [45] A. Gheorghiu, P. Wallden, and E. Kashefi, "Rigidity of quantum steering and one-sided device-independent verifiable quantum computation," *New Journal of Physics*, vol. 19, no. 2, p. 023043, 2017.

- [46] E. N. Gilbert, "Random graphs," *The Annals of Mathematical Statistics*, vol. 30, no. 4, pp. 1141–1144, 1959.
- [47] H. Goto, K. Tatumura, and A. R. Dixon, "Combinatorial optimization by simulating adiabatic bifurcations in nonlinear hamiltonian systems," *Science advances*, vol. 5, no. 4, p. eaav2372, 2019.
- [48] G. G. Guerreschi and A. Y. Matsuura, "Qaoa for max-cut requires hundreds of qubits for quantum speed-up," *Scientific reports*, vol. 9, no. 1, pp. 1–7, 2019.
- [49] M. P. Harrigan, K. J. Sung, M. Neeley, K. J. Satzinger, F. Arute, K. Arya, J. Atalaya, J. C. Bardin, R. Barends, S. Boixo *et al.*, "Quantum approximate optimization of non-planar graph problems on a planar superconducting processor," *Nature Physics*, vol. 17, no. 3, pp. 332–336, 2021.
- [50] R. Herrman, P. C. Lotshaw, J. Ostrowski, T. S. Humble, and G. Siopsis, "Multi-angle quantum approximate optimization algorithm," *Scientific Reports*, vol. 12, no. 1, pp. 1–10, 2022.
- [51] H.-L. Huang, Q. Zhao, X. Ma, C. Liu, Z.-E. Su, X.-L. Wang, L. Li, N.-L. Liu, B. C. Sanders, C.-Y. Lu *et al.*, "Experimental blind quantum computing for a classical client," *Physical review letters*, vol. 119, no. 5, p. 050503, 2017.
- [52] H.-Y. Huang, M. Broughton, J. Cotler, S. Chen, J. Li, M. Mohseni, H. Neven, R. Babbush, R. Kueng, J. Preskill *et al.*, "Quantum advantage in learning from experiments," *Science*, vol. 376, no. 6598, pp. 1182–1186, 2022.
- [53] S. Kumar, H. Zhang, and Y.-P. Huang, "Large-scale ising emulation with four body interaction and all-to-all connections," *Communications Physics*, vol. 3, no. 1, p. 108, 2020.
- [54] J. Li, M. Alam, and S. Ghosh, "Large-scale quantum approximate optimization via divide-and-conquer," *arXiv preprint arXiv:2102.13288*, 2021.
- [55] Q. Li, C. Liu, Y. Peng, F. Yu, and C. Zhang, "Blind quantum computation where a user only performs single-qubit gates," *Optics & Laser Technology*, vol. 142, p. 107190, 2021.
- [56] M. Liang, "Symmetric quantum fully homomorphic encryption with perfect security," *Quantum information processing*, vol. 12, no. 12, pp. 3675–3687, 2013.
- [57] A. Lipowski and D. Lipowska, "Roulette-wheel selection via stochastic acceptance," *Physica A: Statistical Mechanics and its Applications*, vol. 391, no. 6, pp. 2193–2196, 2012.
- [58] S. Lloyd, "Quantum approximate optimization is computationally universal," *arXiv preprint arXiv:1812.11075*, 2018.
- [59] A. Lucas, "Ising formulations of many np problems," *Frontiers in physics*, vol. 2, p. 5, 2014.
- [60] A. Marandi, Z. Wang, K. Takata, R. L. Byer, and Y. Yamamoto, "Network of time-multiplexed optical parametric oscillators as a coherent ising machine," *Nature Photonics*, vol. 8, no. 12, pp. 937–942, 2014.
- [61] C. McGeoch and P. Farre, "The d-wave advantage system: An overview," Tech. Rep. (D-Wave Systems Inc, Burnaby, BC, Canada, 2020), Tech. Rep.
- [62] M. McKague, "Interactive proofs for bqp via self-tested graph states," *arXiv preprint arXiv:1309.5675*, 2013.
- [63] M. E. Morales, J. D. Biamonte, and Z. Zimborás, "On the universality of the quantum approximate optimization algorithm," *Quantum Information Processing*, vol. 19, no. 9, pp. 1–26, 2020.
- [64] T. Morimae and K. Fujii, "Blind quantum computation protocol in which alice only makes measurements," *Physical Review A*, vol. 87, no. 5, p. 050301, 2013.
- [65] H. Nakayama, J. Koyama, N. Yoneoka, and T. Miyazawa, "Description: third generation digital annealer technology," *Fujitsu Limited: Tokyo, Japan*, 2021.
- [66] M. A. Nielsen and I. L. Chuang, *Quantum Computation and Quantum Information*. Cambridge University Press, 2010.
- [67] H. Nishimori and K. Takada, "Exponential enhancement of the efficiency of quantum annealing by non-stoquastic hamiltonians," *Frontiers in ICT*, vol. 4, p. 2, 2017.
- [68] Y. Ouyang, S.-H. Tan, and J. F. Fitzsimons, "Quantum homomorphic encryption from quantum codes," *Physical Review A*, vol. 98, no. 4, p. 042334, 2018.
- [69] W. Peng, B. Wang, F. Hu, Y. Wang, X. Fang, X. Chen, and C. Wang, "Factoring larger integers with fewer qubits via quantum annealing with optimized parameters," *SCIENCE CHINA Physics, Mechanics & Astronomy*, vol. 62, no. 6, p. 60311, 2019.
- [70] D. Pierangeli, G. Marcucci, and C. Conti, "Large-scale photonic ising machine by spatial light modulation," *Physical review letters*, vol. 122, no. 21, p. 213902, 2019.
- [71] M. J. Powell, *A direct search optimization method that models the objective and constraint functions by linear interpolation*. Springer, 1994.
- [72] J. Preskill, "Quantum computing in the nisq era and beyond," *arXiv preprint arXiv:1801.00862*, 2018.
- [73] B. W. Reichardt, F. Unger, and U. Vazirani, "Classical command of quantum systems," *Nature*, vol. 496, no. 7446, pp. 456–460, 2013.
- [74] A. Robert, P. K. Barkoutsos, S. Woerner, and I. Tavernelli, "Resource-efficient quantum algorithm for protein folding," *npj Quantum Information*, vol. 7, no. 1, pp. 1–5, 2021.
- [75] M. Sao, H. Watanabe, Y. Musha, and A. Utsunomiya, "Application of digital annealer for faster combinatorial optimization," *Fujitsu Scientific and Technical Journal*, vol. 55, no. 2, pp. 45–51, 2019.
- [76] A. Sarkar, Z. Al-Ars, and K. Bertels, "Quaser: Quantum accelerated de novo dna sequence reconstruction," *Plos one*, vol. 16, no. 4, p. e0249850, 2021.
- [77] E. Shahamatnia, R. Ayanzadeh, R. A. Ribeiro, and S. Setayeshi, "Adaptive imitation scheme for memetic algorithms," in *Technological Innovation for Sustainability: Second IFIP WG 5.5/SOCOLNET Doctoral Conference on Computing, Electrical and Industrial Systems, DoCEIS 2011, Costa de Caparica, Portugal, February 21-23, 2011. Proceedings 2*. Springer, 2011, pp. 109–116.
- [78] D. Sherrington and S. Kirkpatrick, "Solvable model of a spin-glass," *Physical review letters*, vol. 35, no. 26, p. 1792, 1975.
- [79] P. W. Shor, "Polynomial-time algorithms for prime factorization and discrete logarithms on a quantum computer," *SIAM review*, vol. 41, no. 2, pp. 303–332, 1999.
- [80] A. Shukla, H. M. Pandey, and D. Mehrotra, "Comparative review of selection techniques in genetic algorithm," in *2015 international conference on futuristic trends on computational analysis and knowledge management (ABLAZE)*. IEEE, 2015, pp. 515–519.
- [81] M. Streif, S. Yarkoni, A. Skolik, F. Neukart, and M. Leib, "Beating classical heuristics for the binary paint shop problem with the quantum approximate optimization algorithm," *Physical Review A*, vol. 104, no. 1, p. 012403, 2021.
- [82] K. J. Sung, J. Yao, M. P. Harrigan, N. C. Rubin, Z. Jiang, L. Lin, R. Babbush, and J. R. McClean, "Using models to improve optimizers for variational quantum algorithms," *Quantum Science and Technology*, vol. 5, no. 4, p. 044008, 2020.
- [83] S.-H. Tan, J. A. Kettlewell, Y. Ouyang, L. Chen, and J. F. Fitzsimons, "A quantum approach to homomorphic encryption," *Scientific reports*, vol. 6, no. 1, p. 33467, 2016.
- [84] S. S. Tannu, P. Das, R. Ayanzadeh, and M. K. Qureshi, "Hammer: Boosting fidelity of noisy quantum circuits by exploiting hamming behavior of erroneous outcomes," in *Proceedings of the Twenty-Seventh International Conference on Architectural Support for Programming Languages and Operating Systems*, 2022, pp. 529–540.
- [85] K. Tatumura, A. R. Dixon, and H. Goto, "Fpga-based simulated bifurcation machine," in *2019 29th International Conference on Field Programmable Logic and Applications (FPL)*. IEEE, 2019, pp. 59–66.
- [86] K. Tatumura, M. Yamasaki, and H. Goto, "Scaling out ising machines using a multi-chip architecture for simulated bifurcation," *Nature Electronics*, vol. 4, no. 3, pp. 208–217, 2021.
- [87] T. Trochatos, C. Xu, S. Deshpande, Y. Lu, Y. Ding, and J. Szefer, "Hardware architecture for a quantum computer trusted execution environment," *arXiv preprint arXiv:2308.03897*, 2023.
- [88] P. Vikstål, M. Grönkvist, M. Svensson, M. Andersson, G. Johansson, and G. Ferrini, "Applying the quantum approximate optimization algorithm to the tail-assignment problem," *Physical Review Applied*, vol. 14, no. 3, p. 034009, 2020.
- [89] B. Villalonga, D. Lyakh, S. Boixo, H. Neven, T. S. Humble, R. Biswas, E. G. Rieffel, A. Ho, and S. Mandrà, "Establishing the quantum supremacy frontier with a 281 pflop/s simulation," *Quantum Science and Technology*, vol. 5, no. 3, p. 034003, 2020.
- [90] Y. Wu, W.-S. Bao, S. Cao, F. Chen, M.-C. Chen, X. Chen, T.-H. Chung, H. Deng, Y. Du, D. Fan *et al.*, "Strong quantum computational advantage using a superconducting quantum processor," *arXiv preprint arXiv:2106.14734*, 2021.
- [91] L. Yu, C. A. Pérez-Delgado, and J. F. Fitzsimons, "Limitations on information-theoretically-secure quantum homomorphic encryption," *Physical Review A*, vol. 90, no. 5, p. 050303, 2014.